Editors' Suggestion

# Dzyaloshinskii-Moriya interaction in Ni/Cu(001)

R. Allenspach,[1,*] A. Bischof,[1,†] B. Boehm,[1] U. Drechsler,[1] O. Reich,[1] M. Sousa,[1] S. Tacchi,[2] and G. Carlotti[2,3]

[1]*IBM Research – Zurich, CH-8803 Rüschlikon, Switzerland*

[2]*CNR-IOM, Sede Secondaria di Perugia, c/o Dipartimento di Fisica e Geologia, Università di Perugia, I-06123 Perugia, Italy*

[3]*Dipartimento di Fisica e Geologia, Università di Perugia, I-06123 Perugia, Italy*

(Received 18 April 2024; accepted 11 June 2024; published 1 July 2024)

Dzyaloshinskii-Moriya interaction (DMI) is found in the epitaxial Ni/Cu(001) system by imaging magnetic domain wall profiles with high resolution and by Brillouin light scattering. The domain walls have right-handed chirality and deviate from both the Néel and Bloch configurations for Ni thicknesses up to 9 nm. From a detailed structural analysis it is found that strain in the Ni film is inhomogeneous with film thickness. We suggest that this strain field is responsible for the symmetry breaking that is required for a sizable DMI to appear, even in absence of a heavy metal.

DOI: 10.1103/PhysRevB.110.014402

## I. INTRODUCTION

The Dzyaloshinskii-Moriya interaction (DMI) has gained enormous interest in recent years when it was realized that ultrathin ferromagnets lack inversion symmetry if the combined film/substrate entity is considered. Originally proposed for bulk magnets without centrosymmetry [1,2], this antisymmetric exchange interaction is now explored both for fundamental understanding of magnetic materials and spin textures [3] as well as for possible use in spintronics applications [4].

In ferromagnetic films, the necessary symmetry breaking is achieved by the interface between the ferromagnet and the substrate [5–7]. At this interface, an indirect exchange mechanism is acting between two atoms in the ferromagnet via an atom in the substrate, in addition to direct Heisenberg exchange [4]. Spin-orbit coupling (SOC) is essential for this indirect exchange interaction, but even for large SOC, DMI is only a fraction of standard exchange. Hence, to observe large DMI, almost all experimental studies have been performed with ferromagnets on top of a heavy-metal substrate, as SOC is large in high-Z elements. Moreover, mainly ultrathin ferromagnets (typically thinner than 1–2 nm) were used, so that the interface dominates over the film volume. However, there is also a practical reason why ultrathin films are used: Films should be magnetized out-of-plane. Many ultrathin ferromagnets are perpendicularly magnetized owing to Néel's surface anisotropy, but the competing shape anisotropy eventually rotates the magnetization into the plane by a spin reorientation transition [8,9], taking place typically at a thickness of 1 to 2 nm, depending on the system. There is, however, a noteworthy exception: Ni films epitaxially grown on Cu(001) show a reverse reorientation transition with increasing film thickness. They turn from in-plane to perpendicular magnetization at around 1.5–2 nm, and remain perpendicularly magnetized up to at least 9 nm before they finally return to in-plane magnetization [10,11].

This offers the possibility to investigate DMI in an extended thickness range of a perpendicularly magnetized ferromagnetic film. It is *a priori* by no means clear why the interfacial DMI (i-DMI) concept should be applicable at all for films of such large thicknesses. We therefore decided to explore DMI via the imaging of chiral domain walls in thick Ni films. Additionally, we used a locally averaging technique, Brillouin light scattering (BLS), to compare microscopic and macroscopic information. We complemented these magnetic experiments by a detailed analysis of film growth mode, in order to deduce strain effects in this epitaxial system.

Ferromagnetic Ni epitaxially grown on the Cu(001) surface is a well-studied system, and it proved to be more intricate than what could be naively assumed when a face-centered cubic (fcc) metal is stacked on top of another fcc metal with similar lattice constant. The initial pseudomorphic layer-by-layer growth leads to tensile strain in the film that is gradually relaxed by the formation of misfit dislocations [12,13]. It is remarkable that only a fraction of the strain is removed up to large Ni thicknesses of tens of nanometers. With respect to magnetism, the complexity arises because bulk Ni shows considerable magnetoelastic effects, which are even stronger in thin films as strain modifies the magnetoelastic constants [14]. In fact, the mere existence of the wide thickness range in which Ni/Cu(001) is perpendicularly magnetized is due to bulk magnetoelastic anisotropy [11]. Strain effectively breaks the cubic symmetry along the surface normal, and the Ni film gets tetragonally distorted.

For these reasons we decided to explore if chiral interactions exist in Ni/Cu(001), an epitaxial model

*Contact author: ral@zurich.ibm.com

†Contact author: bis@zurich.ibm.com

*Published by the American Physical Society under the terms of the Creative Commons Attribution 4.0 International license. Further distribution of this work must maintain attribution to the author(s) and the published article's title, journal citation, and DOI.*

system in which no heavy metal is involved and that is perpendicularly magnetized up to thicknesses of about 10 nm.

## II. EXPERIMENTAL METHODS

The Ni films were grown by thermal evaporation on a single-crystalline Cu(001) substrate held at room temperature, with a growth rate of 1–4 nm/h. Some of the samples were grown as a wedge by using a movable shadow mask so that magnetic imaging at different thicknesses was possible on the same sample. Wedges extended typically over a few millimeters, with the Ni thickness varying from 0 to 10 nm. For some experiments, 0.1 nm of Fe was deposited onto Cu before Ni was grown. This "dusting" layer was confined to only part of the sample for direct comparison between Ni/Cu(001) and Ni/Fe/Cu(001). We complemented these experiments by Ni films grown epitaxially on Cu/Si(001). This allows batch-type fabrication of samples and further processing such as cross-sectional focused ion beam milling for structural investigations or magnetometry studies. We followed the recipe that was developed long ago to grow epitaxial Cu on top of Si(001) [15]. We used a Cu thickness of 50 nm, after initially varying the thickness from 15 to 100 nm in order to determine the optimum Cu crystal quality. Evaporation rates were 0.1 nm/s for Cu and 0.2 nm/s for Ni. The Ni/Cu/Si(001) samples were capped by 2 nm of Au to prevent oxidation.

We used our spin-polarized scanning electron microscopy (spin-SEM) tool [16] for magnetic imaging of the samples. With a probing depth of 1 nm, spin-SEM detects the magnetization at the surface of a ferromagnet. Type and chirality of a domain wall (DW) were determined by deducing high-resolution wall profiles of all three magnetization components from these images. In addition to the magnetic images, absorbed current maps were taken simultaneously so that chemical and structural contrast could be related to the magnetic images. As the Ni/Cu/Si(001) samples were grown outside the spin-SEM tool, the Au cap layer was removed after insertion into the tool by $Xe^+$ sputtering. The sputtering process is controlled by monitoring the atomic composition of the surface by Auger electron spectroscopy. The Ni/Cu(001) samples were grown *in situ* and hence did not require sputtering prior to imaging, but Auger spectroscopy was routinely used to determine film thicknesses during growth. The samples were demagnetized before imaging by alternating perpendicular field cycles with gradually decreasing amplitude.

The possible presence of DMI was tested by BLS that was affirmed during the last decade as a popular and reliable technique to quantify the value of the DMI constant $D$ [17]. About 200 mW of a monochromatic laser beam with a wavelength $\lambda = 532$ nm were focused onto the sample surface, using a camera objective of focal length 50 mm corresponding to an illuminated spot of about 40 μm diameter. The same objective was used to collect the backscattered light that was then analyzed in frequency by a Sandercock-type $(3 + 3)$-pass tandem Fabry-Perot interferometer. Measurements were performed in air, at room temperature, on Ni films of thickness 5 nm and 2.7 nm, capped with the above mentioned Au protective overlayer. As is standard practice for measuring interfacial DMI by BLS [17], we exploited the Damon-Eshbach configuration, where an external magnetic field is applied in the sample plane, with an intensity sufficient to saturate the sample, while the wavevector **k** of the revealed spin waves is also in-plane but perpendicular to the magnetic field. Because of the conservation of momentum in the light scattering process, the magnitude of **k** is related to the incidence angle of light $\theta$, by the relation $k = 4\pi \sin\theta/\lambda$. The incidence angle $\theta$ was varied between 10° and 60°. In the presence of DMI, both the Stokes and the anti-Stokes peaks in BLS spectra, corresponding to spin waves propagating with opposite wavevectors, are shifted in frequency by an amount that is proportional to $D$. Note that the sign of $D$ determines the sign of $f_{DMI}$.

We conclude this section by noting that a measured frequency nonreciprocity in BLS by itself is not sufficient to claim a chiral interaction such as DMI. In principle, different surface anisotropies at the two film interfaces also lead to frequency nonreciprocity. However, as clarified in previous studies [18–20], the frequency nonreciprocity due to a difference in surface anisotropies scales with the square of film thickness $d$, i.e., as $d^2$, while the contribution due to DMI scales as $1/d$. Therefore, the nonreciprocity due to surface anisotropy in BLS experiments for films with $d \leqslant$ 6–8 nm, as in the present case, can be disregarded (see for instance Fig. 3 in [18] and Fig. 2 in [19]).

## III. EXPERIMENTAL RESULTS

### A. Analysis of chiral domain walls and quantification of DMI by magnetic imaging

We deduce the DMI of Ni/Cu(001) from magnetic imaging by spin-SEM. By mapping the magnetization vector in areas of the film that contain one or more DWs, we determine the in-plane angle $\varphi$ of the magnetization with respect to the wall normal. This method has been successfully applied before and described in detail [21]. Without DMI, DWs in a perpendicularly magnetized ferromagnet are Bloch walls for stray-field energy reasons and hence $\varphi = 90°$. DMI contributes a term to the wall energy that describes the chiral interaction and leads to the canting of neighboring spins. Depending on the energy balance between DMI and stray-field energy, the in-plane magnetization direction points away from the direction of the Bloch wall. The wall can even become a pure Néel wall with $\varphi = 0°$, provided that DMI is larger than a certain threshold value. Note that with this DW-imaging method, the wall chirality is determined directly without further calculation. The strength of i-DMI is deduced with the help of a model and the material constants of the ferromagnet [21].

In our spin-SEM tool, two components are measured simultaneously. The third component (plus redundantly one of the two other components) can be measured by employing a Wien filter as a spin-rotating device [22]. In this way, we are able to map the magnetization vector with high-resolution across a DW and from the two in-plane components we determine the in-plane magnetization angle $\varphi$. An example is shown in Fig. 1 for 7 nm Ni on Cu(001). In the linescan across the wall, we observe the typical tanh profile for the

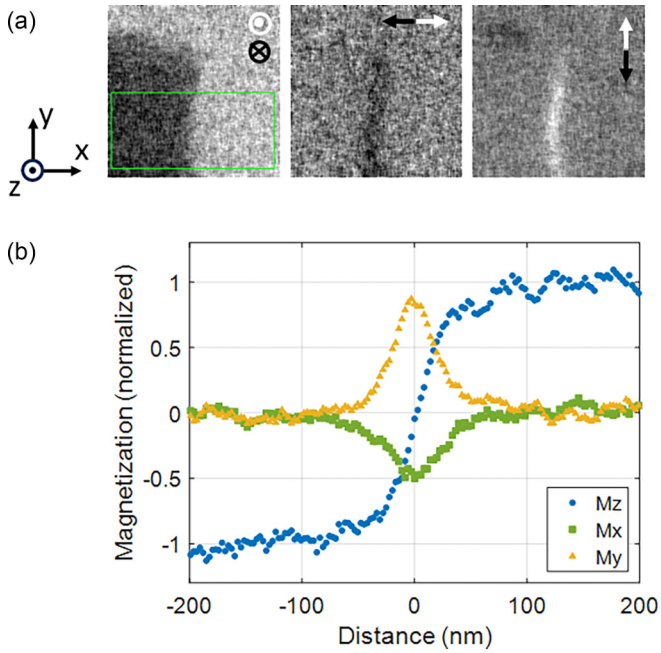


FIG. 1. (a) Spin-SEM images for 7 nm Ni on Cu(001). The three magnetization components $M_z$, $M_x$, $M_y$ are shown in the vicinity of a domain wall. The $M_z$ component identifies the position of the wall, while in the $M_x$ and $M_y$ component a faint contrast is visible within the wall. The wall has right-handed chirality. Image size 460 nm × 460 nm. The images were slightly filtered with a recursive filter to enhance contrast. (b) Linescan across the domain wall for the three components, averaged over the green rectangle indicated in the $M_z$ image in (a). From the ratio of the two in-plane components, $\varphi = 63^\circ$ is calculated.

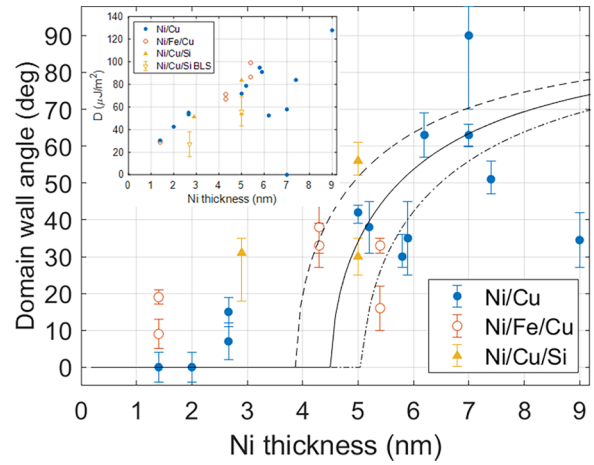


FIG. 2. Domain wall in-plane magnetization angles $\varphi$ vs Ni film thickness $d$ on Cu(001). For $d < 4$ nm, walls are preferentially Néel walls ($\varphi$ close to 0) with right-handed chirality. For larger thicknesses, $\varphi$ increases as the wall gets more and more Bloch-like. The curves are calculated using the model by Lemesh *et al.* [23] assuming interfacial DMI, with an i-DMI constant $D_s$ of +0.3 pJ/m (dashed line), +0.4 pJ/m (solid line), and +0.5 pJ/m (dash-dotted line) as a parameter. The inset shows the effective DMI constant $D$ vs film thickness, calculated from $\varphi$ (for details, see text). The values at $d = 1.4$ and 2 nm should be considered as lower bounds, since no DMI value can be determined if the wall is a pure Néel wall. The DMI values determined by BLS are given for comparison as well.

out-of-plane component $M_z$. As expected for a film with perpendicular anisotropy, the wall is narrow, with a width of 37 ± 3 nm. Both in-plane components $M_x$ and $M_y$ do not vanish within the wall, hence the wall is neither of Bloch nor of Néel type. From the ratio of the maxima of $M_x$ and $M_y$, we deduce an angle $\varphi = 63^\circ$ away from the wall normal. Moreover, the wall has right-handed chirality (or clockwise sense of rotation): When traversing the wall, the magnetization direction rotates from the $+M_z$ into the $-M_z$ direction by pointing towards the $-x$ direction within the wall, in the commonly used right-handed coordinate system.

DW angles measured for Ni thicknesses $d$ up to 9 nm are shown in Fig. 2. We observe that $\varphi$ increases with increasing $d$: For thin films, the wall is essentially of Néel type with $\varphi$ close to 0°, while for thick films, the walls deviate more and more from a Néel wall, getting closer to a Bloch wall. All walls have the same right-handed chirality, consistent with the Dzyaloshinskii-Moriya interaction. To estimate the DMI strength, we use the equation deduced by Lemesh *et al.* [23], which was applied in a similar study [21,24]. DWs are pure Néel walls as long as the DMI strength is larger than a threshold value $D_{\text{thr}} = 2\mu_0 M_s^2 d^2/(\pi^2/ln(2) + \pi d\sqrt{(K_u + \mu_0 M_s^2/2)/A}\,)$. $M_s$ and the uniaxial perpendicular anisotropy $K_u$ were determined by vibrating sample magnetometry (VSM) for a Ni film of 5 nm thickness covered by 2 nm Au: $M_s = 359\,\text{kA/m}$, $K_u = 153\,\text{kJ/m}^3$ (calculated from the anisotropy field $H_A = 320\,\text{kA/m}$). The exchange stiffness $A$ is assumed to correspond to that of bulk Ni, $A = 9\,\text{pJ/m}$. We note that knowing $K_u$ and $A$ is less important: The second term in the denominator becomes relevant for the "ultrathick film" limit [23] and even for films as thick as 5 nm is only a correction of <20%. There is a relatively large spread in the data points, since the measured spin polarization signals in Ni films are notoriously small [25], so the angle determination has a large uncertainty. Moreover, the thickness of the films is only known to within about 10–20% because films were in part grown as flat films and in part as wedges, so the exact position on the wedge matters. And finally, there is never a guarantee in magnetism that the equilibrium lowest energy state is reached by an ac demagnetization procedure. If we assume that DMI is of interfacial origin, we can plot wall magnetization angle vs thickness curves for a fixed i-DMI constant $D_s$. Three model curves are given in Fig. 2 to tentatively estimate $D_s$. We find $D_s = +0.4\,\text{pJ/m}$ but also give the curves corresponding to $D_s = +0.3$ and $+0.5\,\text{pJ/m}$ for comparison. The trend of increasing wall angle with film thickness is reasonably reproduced by the i-DMI model, but agreement is mediocre. The opposite limiting case would be DMI having bulk origin, i.e., each atomic layer of the film contributing equally to DMI. From $\varphi$ we can calculate the effective DMI constant $D$ by noting that $D = D_{\text{thr}}/d$. The inset shows how $D$ varies with $d$. If DMI were a pure bulk effect in Ni/Cu, then $D$ should be constant with $d$. This is not observed and, even more, a clear trend is missing. We postpone a broader discussion to Sec. IV.

Chiral DWs in films with thicknesses up to 9 nm have not been imaged before. And it is surprising that the DMI is

so strong in a ferromagnet on a 3*d* transition metal, as it is believed that a heavy metal with large spin-orbit interaction is a prerequisite for appreciable DMI. For comparison, $D_s = -1$ to $-2$ pJ/m for the prototypical Pt/Co/AlOx system [17,26] or $D_s = +1.07$ pJ/m for Ir/Co [21]. On the other hand, our values are similar to those reported earlier for Ni/Fe/Cu(001) [27–29]. In both studies, however, the DMI was attributed to the Ni/Fe interface and not to the Ni/Cu interface. Chen *et al.* [27] even reported a reversal of the DMI upon reverting Ni and Fe [30] for ultrathin Ni and Fe layers of 0.4 nm thickness each. They also found Bloch walls when Ni was thicker than 2 nm, conflicting with our results.

We investigated the importance of small amounts of Fe at the interface between Ni and Cu(001). The DW angles for Ni films on 0.1 nm Fe/Cu(001) are included in Fig. 2. Within our error margin, we do not find a change of $D_s$, neither in amplitude nor sign. Note that our Ni films are thicker and the Fe dusting layer thinner than in Ref. [27]. In particular, we investigated the thickness range in which the pseudomorphic growth of Ni on Cu(001) is no longer maintained and epitaxial strain becomes relaxed.

### B. Brillouin light scattering

It has been argued that extracting DMI from DWs might be hampered because DWs pin at defects and hence the local, atomic-scale environment at DWs might affect the result [31]. We thus complemented our study with BLS experiments. BLS is rather insensitive to the presence of defects, grain boundaries, or surface roughness, since it involves spin waves with wavelengths of several hundred nanometers, propagating several micrometers along the sample. Hence, BLS averages DMI over the region illuminated by the laser spot, in our case a few tens of micrometers. BLS is able to directly quantify the effective DMI constant by comparing the frequencies of two counter-propagating spin waves, as anticipated in Sec. II. Two Ni thicknesses were investigated, 2.7 nm and 5 nm, grown on 50 nm of Cu on Si(001).

Figure 3 shows the measured frequency difference between the anti-Stokes and the Stokes peaks for the two investigated samples. The effective DMI constant $D$ has been extracted from the slope of the regression lines, according to the linear relation [17]: Slope $= 2\, f_{DMI}/k = 2\gamma D/(\pi M_s)$. The saturation magnetization values were measured by VSM and the gyromagnetic ratio was assumed to be $\gamma = 190$ GHz/T. A positive slope was found for all samples, indicating $D > 0$, i.e., right-handed chirality is favored, in agreement with the spin-SEM observations. The surface constant $D_s$ was then obtained by multiplying $D$ with the film thickness.

The values summarized in Table I are in the range of a fraction of a pJ/m, i.e., similar to the values estimated by the DW analysis.

Such a relatively good agreement between the results obtained by BLS and those by DW analysis should not be taken for granted. In earlier studies in which BLS and DW-expansion experiments were done, either reasonable agreement [32] but also appreciable discrepancy [31,33] was found. It is also not obvious that Ni/Cu(001) and Ni/Cu/Si(001) have exactly the same DMI strength. We therefore repeated the DW analysis by spin-SEM experiments on the Ni/Cu/Si(001) samples. Similar DW angles were found as for the Ni/Cu(001) system, see Fig. 2. We thus conclude for the Ni/Cu system that DMI is not merely confined to the DW locations but extends over the entire sample area.

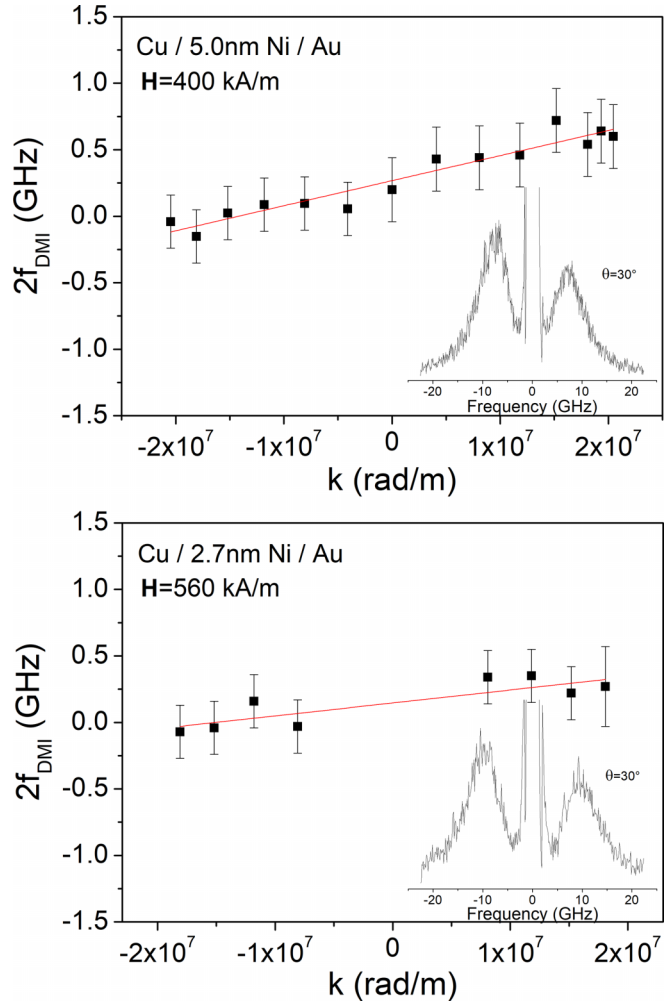


FIG. 3. Measured frequency difference (filled dots) between the anti-Stokes and the Stokes peaks in BLS spectra for the two Ni/Cu/Si(001) films with thickness of 2.7 nm and 5 nm, covered by 2 nm Au. The different data points refer to measurements performed at different angles of incidence, corresponding to different values of the spin wave wavevector $k$. The red lines correspond to the best-fit regression line, whose slope is proportional to the value of the DMI constant $D$. In both panels, the BLS spectrum for $\theta = 30^\circ$ is shown as inset.

### C. Film growth and strain

Let us now consider the strain that develops during epitaxial growth of the Ni film on Cu(001). Since a strain field

TABLE I. Saturation magnetization, effective DMI constant $D$, and surface DMI constant $D_s$ for the two samples analyzed by BLS.

| | $M_s$ (kA/m) | $D$ (μJ/m$^2$) | $D_s$ (pJ/m) |
|---|---|---|---|
| Cu / 5.0 nm Ni / Au | 359 | $56 \pm 13$ | $0.28 \pm 0.10$ |
| Cu / 2.7 nm Ni / Au | 339 | $27 \pm 11$ | $0.07 \pm 0.03$ |

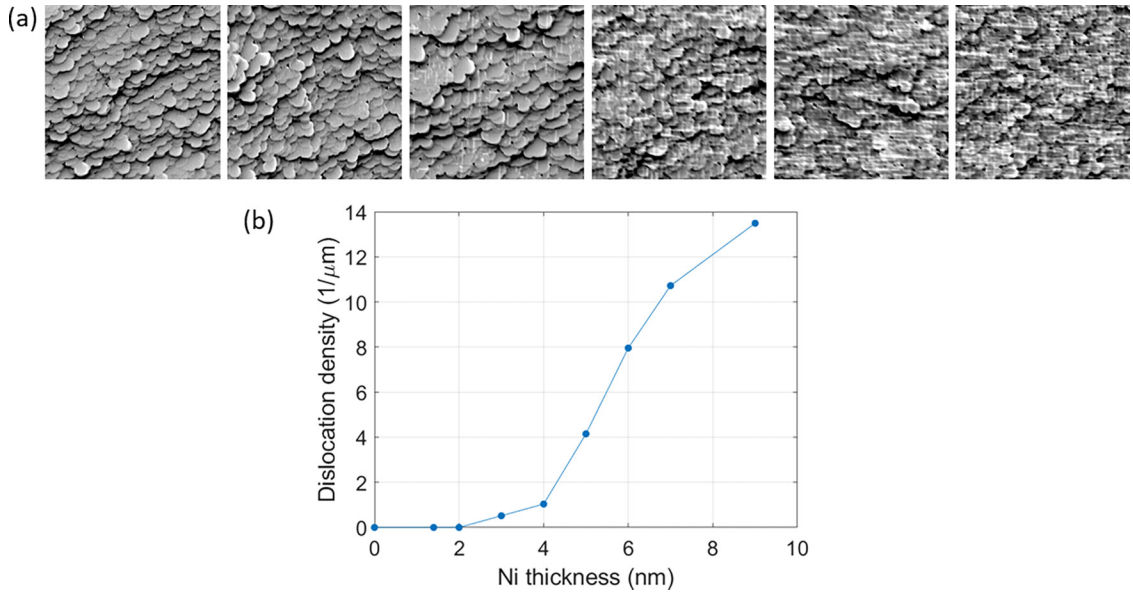


FIG. 4. Dislocation formation in a Ni wedge on Cu(001), as imaged by spin-SEM. (a) Absorbed current images taken along the wedge, showing the steps separating atomically flat terraces and dislocations running along the [110] and [1$\bar{1}$0] directions; Ni thicknesses range from 2 nm (left) to 7 nm (right); image sizes 2.9 μm × 2.9 μm; (b) dislocation density (number of dislocations per micrometer) deduced from the absorbed current images. No dislocations could be identified for $d < 3$ nm.

can break the symmetry along the sample normal, it could contribute to DMI, as we will discuss in Sec. IV below.

The growth of Ni on Cu has been investigated extensively [12–15,34,35]. Up to at least 2 nm, Ni grows pseudomorphically on Cu(001), with the in-plane lattice constant being expanded by 2.5% to adopt the Cu lattice [15]. As a consequence, the out-of-plane lattice constant is shrunk by 3.2% to minimize the elastic energy and hence Ni is tetragonally distorted [11]. With increasing thickness, the lattice strain relaxes by introducing misfit dislocations, as observed decades ago [12,13]. A simple model predicts that strain relaxes with film thickness $d$ as $1/d$ [36]. However, Ni films up to thicknesses of at least 10 nm are under considerable tensile strain [12,14], considerably larger than what is expected from this model.

In our spin-SEM tool, we observe dislocation formation simultaneously with magnetic imaging. The misfit dislocation glide planes appear in the absorbed current image as bright straight lines along the [110] and [1$\bar{1}$0] directions. Figure 4 shows a series of such images taken on a Ni wedge. The dislocation density increases with increasing Ni thickness, reflecting the fact that strain is relieved more and more by introducing additional dislocations. A determination of film strain in Ni on Cu(001) directly from dislocation densities is hampered by the fact that the energy barriers might hinder the formation of dislocations in complex ways. Cantilever bending experiments and x-ray diffraction have been used to deduce average film strain [14,15]. Both report that a considerable tensile strain remains in the film up to at least $d = 10$ nm.

These experiments reveal average strain values. However, it would be beneficial to know the strain profile across the Ni film. For this, we performed high-resolution scanning transmission electron microscopy (STEM) and energy-dispersive x-ray spectroscopy (EDS) on a cross section of a 5 nm Ni film deposited on 50 nm Cu/Si(001) to investigate growth mode and strain in the Ni film. The sample was capped with 2 nm of Au. The cross-section lamellae for the STEM investigations were prepared in a focused ion-beam (FIB) tool.

The bright-field STEM image in Fig. 5(a) displays the well-resolved atomic lattice structures of Cu and Ni, while the interface between the two cannot be identified easily due to a lack of contrast since the elemental masses of Ni and Cu are very similar. To locate the interface, EDS linescans across the sample were performed, see Fig. 5(b). The interface appears to be intermixed in a thickness range of <1.2 nm. This is an upper limit, since some nonorthogonal alignment of the crystal growth facets in the STEM setup could be responsible for the gradual transition to some extent. In order to evaluate the strain in the Ni film, we determine the in-plane lattice constant of the sample (i.e., parallel to the interface) by fast Fourier transforms as a function of the distance from the interface, see Fig. 5(b). The in-plane lattice constant is found to gradually decrease in Ni with increasing distance from the interface, being 0.6% smaller at the top of the film than the Cu bulk lattice constant. This means that it is still considerably larger than the bulk lattice constant of Ni. Hence, despite the fact that a 5 nm Ni film relaxes strain by dislocation formation, tensile strain is large and gradually changes with distance from the Cu substrate. This also means that the out-of-plane lattice constant will gradually change with distance from the interface, since the volume of the Ni unit cell is maintained. We have not investigated whether this behavior also holds for ultrathin Ni films in the pseudomorphic growth regime. According to a LEED study, strain is essentially homogeneous across a 2 nm Ni film [34]. Strain within the film plane will also be inhomogeneous, as misfit will preferentially be concentrated around the dislocations. This could have consequences on our method to determine DMI strength from the DW angle, since the domain wall is confined to specific positions and directions within the crystal structure. Figure 6 displays DWs in 4.3 nm Ni on 0.1 nm Fe/Cu(001). At this thickness, the dislocation

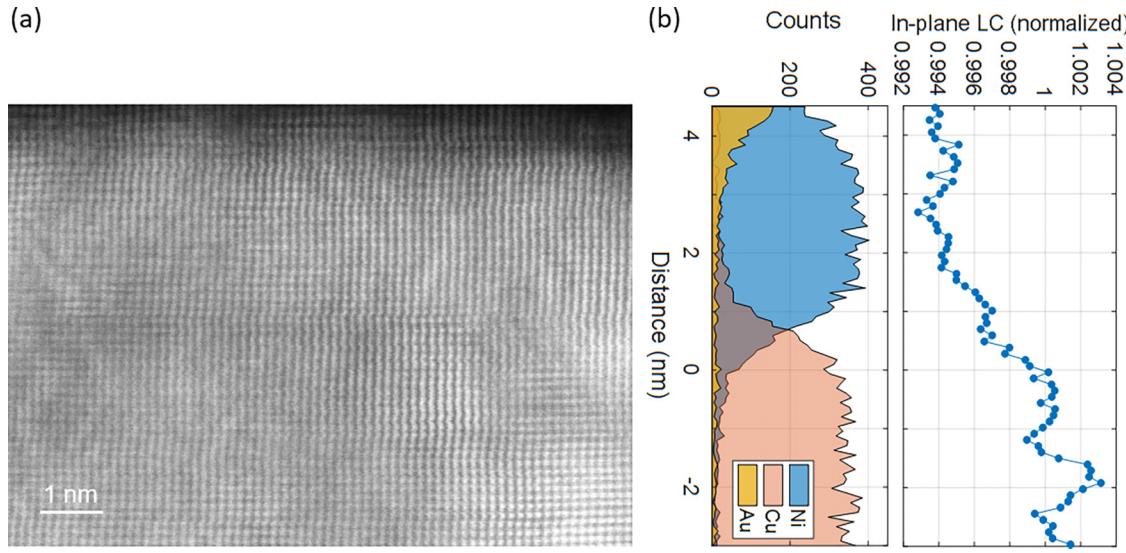


FIG. 5. (a) Bright-field STEM image of 5 nm Ni on Cu/Si(001), covered by 2 nm of Au. (b) EDS elemental profiles and in-plane lattice constant (LC) across the sample, normalized to the Cu lattice constant, as calculated by FFT analysis of the image shown in (a). A gradual change of lattice constant is observed. The Ni lattice is strained inhomogeneously with the film thickness.

lines are clearly visible in the absorbed current image and spaced apart enough so that one can distinguish if a wall is pinned at a dislocation or not. We do not observe an effect on the wall angle within the statistical error: $\varphi = 35 \pm 5^\circ$ for the wall pinned at a dislocation, and $\varphi = 33 \pm 6^\circ$ and $38 \pm 7^\circ$ for the walls where no dislocation can be identified. What we observe, however, is that the wall width is about a factor of 3 smaller when the wall is pinned. This could mean that the position of a DW can fluctuate if pinning is not strong enough [37].

## IV. DISCUSSION

Our results on the Ni/Cu(001) system reveal two striking observations: (i) DMI is considerable, even in films as thick as 9 nm, and (ii) strain is inhomogeneous and only partly relaxed even in the thickest films.

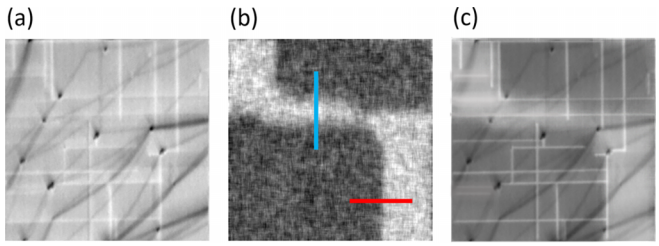


FIG. 6. Spin-SEM images of a 1.4 μm × 1.4 μm area in a 4.3-nm Ni film on Cu(001), with 0.1-nm Fe at the interface between Cu and Ni. (a) Absorbed current image; dislocations are visible as bright lines and single defects as dark indents. (b) Perpendicular magnetization component with a straight narrow DW pinned exactly at a dislocation and two wider walls whose ends are pinned at single defects but the walls do not run parallel to a dislocation line. The wall angle $\varphi$ is 35° for the wall pinned at the dislocation (line profile taken at red line) and $\varphi = 33^\circ$ and $\varphi = 38^\circ$ for the walls where no dislocation is present (line profile taken at blue line includes two walls). To visualize the location of the domain walls with respect to the dislocations, the images (a) and (b) are superimposed in (c).

Observation (i) leads us to question whether the interfacial DMI model is appropriate for the Ni/Cu system, also because the i-DMI model does not reproduce the wall angles in Fig. 2 well. Moreover, Cu is a substrate that is not known for providing large SOC. Despite this, it has been reported that i-DMI is substantial for ultrathin Ni/Fe and Fe/Ni stacks on Cu [27,30]. It should drop off rapidly with film thickness, but there is in principle no upper thickness at which it will completely disappear. The achiral Bloch wall with $\varphi = 90^\circ$ is reached exactly only at infinite thickness, at least under the assumption that the minimum energy state is indeed reached. The threshold thickness, below which the DW has exclusively Néel character, is according to Fig. 2 on the order of 3–4 nm. Also, this is large when compared with, e.g., Co/Pt or Co/Ir, even considering that one can expect it to be somewhat larger for Ni than for Co, since DMI scales with the square of the magnetization [23,38]. Hence, we argue that i-DMI cannot explain our observations entirely.

Recently, DMI has been identified in GdFeCo ferrimagnetic alloys in thick films up to 50 nm [39,40]. DMI was found to increase linearly with film thickness, from which it was concluded that bulk-DMI must be acting. Moreover, i-DMI is unlikely to contribute in Ref. [39] since the DMI value would lead to an interfacial $D_s$ that is larger than any value found so far in ultrathin films, while in Ref. [40], DMI was very small and only observable because of the strongly reduced $M_s$ in this material near the compensation point. The observed DMI was in both studies attributed to an elemental composition gradient across the film, identified by electron energy-loss spectroscopy elemental profiles. No heavy-metal substrate was involved. Gd was proposed to take the role of the element that supplies large SOC through its 5*d* electrons. A layer-resolved Monte Carlo simulation puts these observations on more general grounds and suggests that both chirality and strength of the DMI can be tuned by tuning the

elemental composition, even in disordered systems. To signify that this interaction is different from a standard bulk-DMI, it was called gradient-DMI (g-DMI) [41]. However, also in these simulations, one of the atomic species involved is assumed to have large SOC for efficient DMI. Based on our EDS data shown in Fig. 5(b), a compositional gradient might extend at maximum over a thickness range of 1.2 nm at the Cu/Ni interface. Moreover, no large-SOC element is involved that could efficiently supply a considerable effect. We therefore conclude that g-DMI is of minor importance in the Ni/Cu system.

What is then the origin of the chiral effects we observe in Ni/Cu? Let us consider observation (ii) above: Figure 5(b) shows a gradient in strain, and even in thick Ni films only a fraction of the lattice mismatch is relaxed. The strain gradient across the film thickness is breaking the inversion symmetry, fulfilling the basic requirement for DMI to exist. Indeed, when i-DMI was still in its infancy, Bogdanov and Rössler proposed that chiral interactions can in general be induced by strain effects, and they even proposed Ni/Cu(001) as a convenient system to observe such effects [42]. Combining *ab initio* density functional theory calculations with micromagnetic simulations, Beck and Fähnle found that the DMI strength scales linearly with strain in a bilayer of Fe on W(110) [43]. They argue though that the effect should be small. Given that "standard" i-DMI in Fe/W(110) is acting strongly at the interface, a possible strain effect might be hard to discover experimentally in this system. Strain leading to DMI was also tentatively considered to explain asymmetric vortex switching in $Ni_{80}Fe_{20}$ films, but no further evidence was provided [44]. Recently, it was found by a systematic analysis of the symmetries of all point groups that inhomogeneous strain leads to DMI in any material class, even without inversion symmetry [45]. These symmetry arguments cannot estimate the size of the effect but they predict that for fcc-Ni with its $m\bar{3}m$ point group, a cycloidic interaction is expected, consistent with our observations of chiral Néel walls. Experimental proof for the predictions of Ref. [45] was given very recently in thick centrosymmetric $La_{0.67}Sr_{0.33}MnO_3$ films grown on $NdGaO_3$, with convincing agreement between measured strain gradient and spin-wave frequency shift [46]. The manganite system is rather complex with three nonvanishing orthogonal DMI components and both helicoidal and cycloidal interactions. In comparison, our Ni/Cu system is simpler with its fourfold in-plane symmetry: Inhomogeneous strain leads to an in-plane DMI vector and a cycloidal texture only.

We are not able to quantify the effects of strain on the DMI strength, as this would require sophisticated relativistic calculations. As for all flavors of DMI, large SOC helps to observe the effects. Neither the Ni nor the Cu atom fulfills this requirement. The tetragonally distorted Ni/Cu system, on the other hand, has a significant orbital moment of $0.06\,\mu_B$, compared to a spin moment of $0.56\,\mu_B$ [47]. DMI effects can be observed if the ratio of DMI and exchange is reasonably large, and this ratio scales with the ratio of the orbital-to-spin moment [42], which amounts to 10%. It should also be mentioned that the mere fact of Ni/Cu having perpendicular magnetic anisotropy is proof that spin-orbit interaction is not negligible in this system, since perpendicular magnetic anisotropy is to good approximation proportional to the square of the spin-orbit coupling [48]. If film strain then changes the magnetoelastic coupling coefficients, orbital moments will also be changed.

For the large part of the Ni film, we suggest that a strain-induced DMI is acting, which we call s-DMI. Such an s-DMI affects the entire Ni film and hence should in principle behave as a bulk effect, similar to g-DMI. Strain relaxation by formation of misfit dislocations indeed affects the entire film thickness. A typical strain relaxation vs film thickness curve, however, decays with the inverse of the thickness [36]. Hence, one could expect that the bulk-like strain-induced DMI is disguised as an interfacial DMI, similar to what occurs in the $Co_2FeAl$ films investigated in Ref. [49]. This will hold only approximately, since the $1/d$ dependence does not describe reality well in the Ni/Cu system, as shown by stress measurements during Ni deposition [14]. This agrees with the observation in the manganite films that the DMI strength neither scales as a bulk nor as an interface effect with film thickness [46]. In Ni/Cu, the decay is much less pronounced, as shown by stress measurements during Ni deposition [14].

In view of these considerations, let us revisit Fig. 2. The general trend of increasing wall angle with film thickness is reproduced by the i-DMI model, but overall agreement is moderate. It was proposed that the model can be extended to include bulk-DMI [23], but the the proposed DMI term favors helicoidal Bloch walls instead of cycloidal Néel walls because of the symmetry of the underlying DMI term, conflicting with our findings. According to our data, DMI is also not constant, not even in the pseudomorphic growth regime for $d < 3$ nm (see inset of Fig. 2). A term compatible with the point group symmetry of strained tetragonal Ni films [45] could be added to a DMI model. Such a term has exactly the same functional dependence as the i-DMI term but is of s-DMI origin. We hence argue that a further interfacial-like term would be required to model the Ni/Cu(001) system. Adding further parameters does in general improve agreement with experimental data, but will not provide further insight.

## V. CONCLUSIONS

In conclusion, we find chiral domain walls in perpendicularly magnetized films as thick as 9 nm in the Ni/Cu(001) epitaxial system. This is all the more remarkable since DMI in thin films is believed to originate from the spin-orbit interaction at the interface between substrate and film, and since both substrate and film are $3d$ transition metal elements, spin-orbit interaction is considerably smaller than in prototypical DMI systems. By atomic-scale structural analysis we find that the Ni films are under tensile strain and that this strain is only partly relaxed by misfit dislocations. We argue that the inhomogeneity of this strain leads to an effective DMI, despite the fact that only $3d$ transition metals are involved. By employing a microscopic and a macroscopic technique to determine DMI strength, we can prove that DMI is not only present in strongly strained regions of the film near dislocations but extends over the entire sample area. The sign and strength of DMI is preserved by adding dusting layers of Fe at the interface and/or

at the surface, indicating that it is not the interface but the volume part of the film that is responsible for the chiral effects found in Ni/Cu(001).

## ACKNOWLEDGMENTS

We are grateful to Teruo Kohashi for discussions and insight into constructing a spin rotator. The research leading to these results has received funding from the European Union Seventh Framework Programme [FP7-People-2012-ITN] under grant agreement 316657 (SpinIcur), the European Union's Horizon 2020 Programme FET-Open under grant agreement 861618 (SpinEngine) and by the European Union - NextGenerationEU under the Italian Ministry of University and Research (MUR) National Innovation Ecosystem grant ECS00000041 - VITALITY - CUP: Nos. J97G22000170005 and B43C22000470005. Acknowledgment to PRIN 2022 "Metrology for spintronics: A machine learning approach for the reliable determination of the Dzyaloshinskii-Moriya interaction (MetroSpin)", 2022SAYARY.

[1] I. Dzyaloshinskii, A thermodynamic theory of "weak" ferromagnetism of antiferromagnetics, J. Phys. Chem. Solids **4**, 241 (1958).

[2] T. Moriya, Anisotropic superexchange interaction and weak ferromagnetism, Phys. Rev. **120**, 91 (1960).

[3] R. E. Camley and K. L. Livesey, Consequences of the Dzyaloshinskii-Moriya interaction, Surf. Sci. Rep. **78**, 100605 (2023).

[4] A. Fert, V. Cros, and J. Sampaio, Skyrmions on the track, Nat. Nanotechnol. **8**, 152 (2013).

[5] A. R. Fert, Magnetic and transport properties of metallic multilayers, Mater. Sci. Forum **59-60**, 439 (1990).

[6] A. Crépieux and C. Lacroix, Dzyaloshinsky-Moriya interactions induced by symmetry breaking at a surface, J. Magn. Magn. Mater. **182**, 341 (1998).

[7] M. Heide, G. Bihlmayer, and S. Blügel, Dzyaloshinskii-Moriya interaction accounting for the orientation of magnetic domains in ultrathin films: Fe/W(110), Phys. Rev. B **78**, 140403(R) (2008).

[8] D. P. Pappas, K.-P. Kamper, and H. Hopster, Reversible transition between perpendicular and in-plane magnetization in ultrathin films, Phys. Rev. Lett. **64**, 3179 (1990).

[9] R. Allenspach and A. Bischof, Magnetization direction switching in Fe/Cu(100) epitaxial films: Temperature and thickness dependence, Phys. Rev. Lett. **69**, 3385 (1992).

[10] R. Jungblut, M. T. Johnson, J. aan de Stegge, A. Reinders, and F. J. A. den Broeder, Orientational and structural dependence of magnetic anisotropy of Cu/Ni/Cu sandwiches: Misfit interface anisotropy, J. Appl. Phys. **75**, 6424 (1994).

[11] B. Schulz and K. Baberschke, Crossover from in-plane to perpendicular magnetization in ultrathin Ni/Cu(001) films, Phys. Rev. B **50**, 13467 (1994).

[12] J. W. Matthews and J. L. Crawford, Accommodation of misfit between single-crystal films of nickel and copper, Thin Solid Films **5**, 187 (1970).

[13] D. Mitlin, A. Misra, T. E. Mitchell, J. P. Hirth, and R. G. Hoagland, Interface dislocation structures at the onset of coherency loss in nanoscale Ni-Cu bilayer films, Philos. Mag. **85**, 3379 (2005).

[14] D. Sander, The magnetic anisotropy and spin reorientation of nanostructures and nanoscale films, J. Phys.: Condens. Matter **16**, R603 (2004).

[15] Chin-an Chang, Reversed magnetic anisotropy in deformed (100) Cu/Ni/Cu structures, J. Appl. Phys. **68**, 4873 (1990).

[16] R. Allenspach, Spin-polarized scanning electron microscopy, IBM J. Res. Dev. **44**, 553 (2000).

[17] M. Kuepferling, A. Casiraghi, G. Soares, G. Durin, F. Garcia-Sanchez, L. Chen, C. H. Back, C. H. Marrows, S. Tacchi, and G. Carlotti, Measuring interfacial Dzyaloshinskii-Moriya interaction in ultrathin magnetic films, Rev. Mod. Phys. **95**, 015003 (2023).

[18] O. Gladii, M. Haidar, Y. Henry, M. Kostylev, and M. Bailleul, Frequency nonreciprocity of surface spin wave in permalloy thin films, Phys. Rev. B **93**, 054430 (2016).

[19] O. Gladii, M. Collet, Y. Henry, J.-V. Kim, A. Anane, and M. Bailleul, Determining key spin-orbitronic parameters via propagating spin waves, Phys. Rev. Appl. **13**, 014016 (2020).

[20] A. A. Stashkevich, M. Belmeguenai, Y. Roussigné, S. M. Cherif, M. Kostylev, M. Gabor, D. Lacour, C. Tiusan, and M. Hehn, Experimental study of spin-wave dispersion in Py/Pt film structures in the presence of an interface Dzyaloshinskii-Moriya interaction, Phys. Rev. B **91**, 214409 (2015).

[21] F. Kloodt-Twesten, S. Kuhrau, H. P. Oepen, and R. Frömter, Measuring the Dzyaloshinskii-Moriya interaction of the epitaxial Co/Ir(111) interface, Phys. Rev. B **100**, 100402(R) (2019).

[22] T. Kohashi, H. Matsuyama, and K. Koike, A spin rotator for detecting all three magnetization vector components by spin-polarized scanning electron microscopy, Rev. Sci. Instrum. **66**, 5537 (1995).

[23] I. Lemesh, F. Büttner, and G. S. D. Beach, Accurate model of the stripe domain phase of perpendicularly magnetized multilayers, Phys. Rev. B **95**, 174423 (2017).

[24] See the Supplemental Material of Ref. [21] for a thorough discussion of the model. We note that the formula for $D_{\mathrm{thr}}$ written in the text is proportional to $d^2$ and hence is a surface term (typical units pJ/m). Dividing by $d$ leads to the equally often used effective DMI threshold (typical units $\mu\mathrm{J}/\mathrm{m}^2$).

[25] R. Allenspach, in *Modern Techniques for Characterizing Magnetic Materials*, edited by Y. Zhu (Springer, New York, 2005), p. 329.

[26] M. Belmeguenai, J.-P. Adam, Y. Roussigné, S. Eimer, T. Devolder, J.-V. Kim, S. M. Cherif, A. Stashkevich, and A. Thiaville, Interfacial Dzyaloshinskii-Moriya interaction in perpendicularly magnetized Pt/Co/AlOx ultrathin films measured by Brillouin light spectroscopy, Phys. Rev. B **91**, 180405(R) (2015).

[27] G. Chen, T. Ma, A. T. N'Diaye, H. Kwon, C. Won, Y. Wu, and A. K. Schmid, Novel chiral magnetic domain wall structure in Fe/Ni/Cu(001) films, Phys. Rev. Lett. **110**, 177204 (2013).

[28] T. N. G. Meier, M. Kronseder, and C. H. Back, Domain-width model for perpendicularly magnetized systems with

Dzyaloshinskii-Moriya interaction, Phys. Rev. B **96**, 144408 (2017).

[29] M. Robertson, C. J. Agostino, G. Chen, S. P. Kang, A. Mascaraque, E. G. Michel, C. Won, Y. Wu, A. K. Schmid, and K. Liu, In-plane Néel wall chirality and orientation of interfacial Dzyaloshinskii-Moriya vector in magnetic films, Phys. Rev. B **102**, 024417 (2020).

[30] The sign of the DMI reported in Ref. [27] was inverted in a later publication [29] for Fe/Ni/Cu(001). Correspondingly, the assignment of the wall chirality in Ni/Fe/Cu(001) needs to be corrected to right-handed, as confirmed by A. K. Schmid, co-author of Ref. [27].

[31] R. Soucaille, M. Belmeguenai, J. Torrejon, J.-V. Kim, T. Devolder, Y. Roussigné, S.-M. Chérif, A. A. Stashkevich, M. Hayashi, and J.-P. Adam, Probing the Dzyaloshinskii-Moriya interaction in CoFeB ultrathin films using domain wall creep and Brillouin light spectroscopy, Phys. Rev. B **94**, 104431 (2016).

[32] K. Shahbazi, J.-V. Kim, H. T. Nembach, J. M. Shaw, A. Bischof, M. D. Rossell, V. Jeudy, T. A. Moore, and C. H. Marrows, Domain-wall motion and interfacial Dzyaloshinskii-Moriya interactions in Pt/Co/Ir($t_{Ir}$)/Ta multilayers, Phys. Rev. B **99**, 094409 (2019).

[33] A. Magni, G. Carlotti, A. Casiraghi, E. Darwin, G. Durin, L. Herrera Diez, B. J. Hickey, A. Huxtable, C. Y. Hwang, G. Jakob *et al.*, Key points in the determination of the interfacial Dzyaloshinskii-Moriya interaction from asymmetric bubble domain expansion, IEEE Trans. Magn. **58**, 4002616 (2022).

[34] W. Platow, U. Bovensiepen, P. Poulopoulos, M. Farle, K. Baberschke, L. Hammer, S. Walter, S. Müller, and K. Heinz, Structure of ultrathin Ni/Cu(001) films as a function of film thickness, temperature, and magnetic order, Phys. Rev. B **59**, 12641 (1999).

[35] R. Naik, C. Kota, J. S. Payson, and G. L. Dunifer, Ferromagnetic-resonance studies of epitaxial Ni, Co, and Fe films grown on Cu(100)/Si(100), Phys. Rev. B **48**, 1008 (1993).

[36] C. Chappert and P. Bruno, Magnetic anisotropy in metallic ultrathin films and related experiments on cobalt, J. Appl. Phys. **64**, 5736 (1988).

[37] M. Kronseder, T. N. G. Meier, M. Zimmermann, M. Buchner, M. Vogel, and C. H. Back, Real-time observation of domain fluctuations in a two-dimensional magnetic model system, Nat. Commun. **6**, 6832 (2015).

[38] A. Thiaville, S. Rohart, É. Jué, V. Cros, and A. Fert, Dynamics of Dzyaloshinskii domain walls in ultrathin magnetic films, Europhys. Lett. **100**, 57002 (2012).

[39] D.-H. Kim *et al.*, Bulk Dzyaloshinskii-Moriya interaction in amorphous ferrimagnetic alloys, Nat. Mater. **18**, 685 (2019).

[40] S. Krishnia, E. Haltz, L. Berges, L. Aballe, M. Foerster, L. Bocher, R. Weil, A. Thiaville, J. Sampaio, and A. Mougin, Spin-orbit coupling in single-layer ferrimagnets: Direct observation of spin-orbit torques and chiral spin textures, Phys. Rev. Appl. **16**, 024040 (2021).

[41] J. Liang, M. Chshiev, A. Fert, and H. Yang, Gradient-induced Dzyaloshinskii-Moriya interaction, Nano Lett. **22**, 10128 (2022).

[42] A. N. Bogdanov and U. K. Rössler, Chiral symmetry breaking in magnetic thin films and multilayers, Phys. Rev. Lett. **87**, 037203 (2001).

[43] P. Beck and M. Fähnle, Dzyaloshinskii-Moriya interactions in systems with fabrication induced strain gradients: An ab-initio study, J. Magn. Magn. Mater. **322**, 3701 (2010).

[44] M. Curcic, B. Van Waeyenberge, A. Vansteenkiste, M. Weigand, V. Sackmann, H. Stoll, M. Fähnle, T. Tyliszczak, G. Woltersdorf, C. H. Back, and G. Schütz, Polarization selective magnetic vortex dynamics and core reversal in rotating magnetic fields, Phys. Rev. Lett. **101**, 197204 (2008).

[45] D. A. Kitchaev, I. J. Beyerlein, and A. Van der Ven, Phenomenology of chiral Dzyaloshinskii-Moriya interactions in strained materials, Phys. Rev. B **98**, 214414 (2018).

[46] Y. Zhang *et al.*, Strain-driven Dzyaloshinskii-Moriya interaction for room-temperature magnetic skyrmions, Phys. Rev. Lett. **127**, 117204 (2021).

[47] J. Okabayashi, Y. Miura, and T. Taniyama, Strain-induced reversible manipulation of orbital magnetic moments in Ni/Cu multilayers on ferroelectric $BaTiO_3$, npj Quantum Mater. **4**, 21 (2019).

[48] D. S. Wang, R. Wu, and A. J. Freeman, First-principles theory of surface magnetocrystalline anisotropy and the diatomic-pair model, Phys. Rev. B **47**, 14932 (1993).

[49] M. Belmeguenai, M. S. Gabor, Y. Roussigné, T. Petrisor Jr., R. B. Mos, A. Stashkevich, S. M. Chérif, and C. Tiusan, Interfacial Dzyaloshinskii-Moriya interaction sign in Ir/$Co_2$FeAl systems investigated by Brillouin light scattering, Phys. Rev. B **97**, 054425 (2018).